ChemPubSoc Europe

DOI: 10.1002/slct.201600687

Chemistry SELECT Communications

Materials Science inc. Nanomaterials & Polymers

The Effect of Hydrophobicity on the Synthesis of Homogeneous and Nanostructured NiMo-Based Hybrid Materials

Benjamin Farin, Michel Devillers, and Eric M. Gaigneaux*[a]

Nanostructured hybrid materials made of guest ions and a polyampholytic self-assembled copolymer are here synthesized. Their lamellar organization results from hydrophobic interactions between the copolymer alkyl side chains. Longer side chains improve the organization of hybrids what makes them more attractive to be used as a template for the preparation of sophisticated catalysts. However, they also enhance the hydrophobicity of the copolymer what complicates the synthesis of such hybrids. Dodecyl side chains appear as a compromise that enables to prepare well organized hybrids without sacrificing the copolymer capacity to link ions.

The development of hybrid materials associating organic and inorganic components has become a major concern as it offers the possibility to combine specific properties and features of various components within one material[1]. For several decades, a huge diversity of compounds has already been exploited to design highly sophisticated materials with applications in numerous technological areas like water depollution[2], medicine[3], optics[4], electronics[5] and catalysis[6]. In this work, hybrid materials made of guest inorganic ions (Ni cations and Mo-based anions) and a polyampholytic self-assembled copolymer were prepared. They are dedicated to be used as precursors for the synthesis of bulk NiMo-based oxides presenting properties responsible for improved catalytic performances[7]. While non-porous materials are generally produced, nanostructured and mesoporous $NiMoO_4$ are especially targeted here. In line with preliminary works carried out on the use of similar matrixes for the synthesis of bulk pure or mixed (solid solutions) Ni, Co and Mn molybdates, the used copolymer results from the alternated copolymerization of a diallyl ammonium salt with maleic acid[8]. It possesses tuneable side chains of 6 (C6 matrix), 12 (C12 matrix) or 18 (C18 matrix) carbon atoms fixed to each diallylamine group and presents a lamellar organization thanks to hydrophobic interactions between the side chains (Figure 1)[8a]. This assumption is motivated by the presence of a low-angle peak of Bragg on the copolymer X-ray diffractograms (Figure 2). By using the Bragg law ($2d\sin\theta = n\lambda$), the position of this

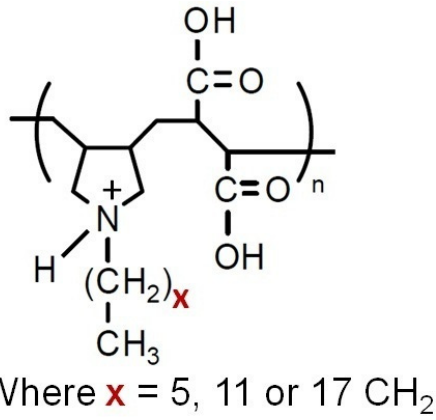

Figure 1. Repeating unit of the copolymer poly[N,N-diallyl-N-alkylamine-alt-(maleic acid)].

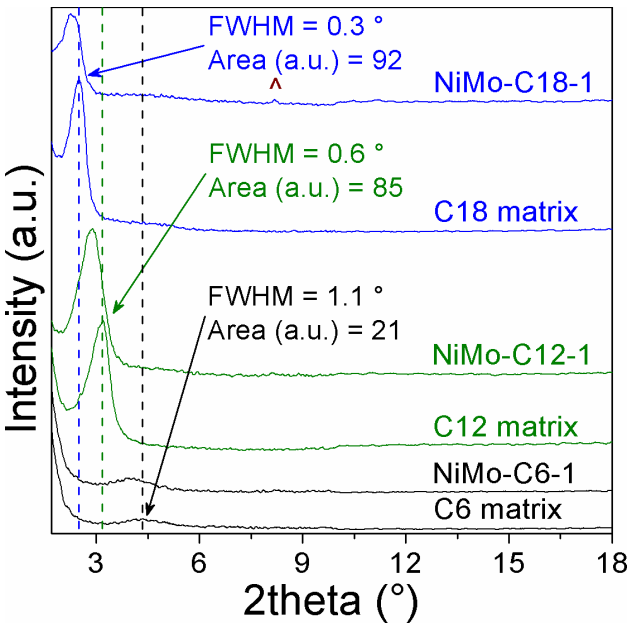

Figure 2. Diffractograms of the copolymer matrices and hybrid materials having an I/R ratio = 1. $(NH_4)_4[NiMo_6O_{18}(OH)_6]\cdot 5H_2O$ ( ) was identified.

[a] *B. Farin, Prof. Dr. M. Devillers, Prof. Dr. E. M. Gaigneaux*
Institute of Condensed Matter and Nanosciences (IMCN)
"Université catholique de Louvain (UCL)"
Place Louis Pasteur, 1 box L4.01.09, 1348 Louvain-la-Neuve (Belgium)
E-mail: eric.gaigneaux@uclouvain.be

Supporting information for this article is available on the WWW under http://dx.doi.org/10.1002/slct.201600687

peak indicates an interreticular distance (d_{Bragg}) repeated along the copolymer structuration (19.8, 27.8 and 34.8 Å for the C6, C12 and C18 matrix respectively)[9]. Such a lamellar organization can be conceptualized as the alternation of hydrophobic and hydrophilic regions[8a,9]. Preserving this organization within the hybrids is crucial to exploit this copolymer as a template agent. During the calcination, the burning of the hydrophobic regions is expected to liberate a volume for the creation of pores[10]. In fact, this strategy assumes that the properties of a catalyst are at least partly dictated by the nanoscopic features of the precursor from which it comes from.

In this context, the length of the alkyl side chains is the key parameter. The side chains do not exist in the all trans conformation mode as the asymmetric stretching band (ν_{as}^{CH2}) of the CH_2 groups is never observed between 2916 and 2920 cm^{-1} (Figure 3)[11]. However, increasing their length progressively

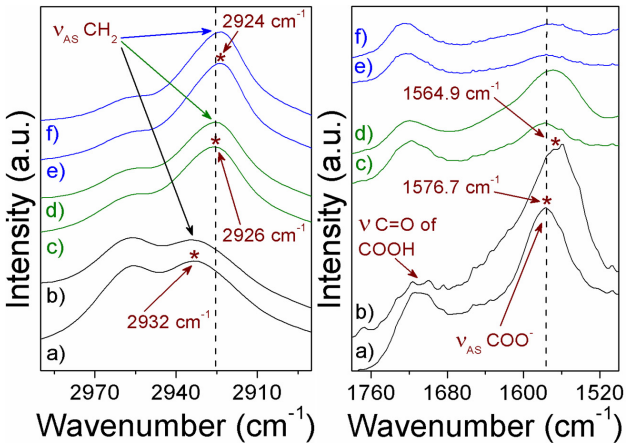

Figure 3. FTIR spectra (between 2990–2890 cm^{-1} on the left side and between 1780–1500 cm^{-1} on the right side) of the C6 matrix (a), the NiMo–C6-1 hybrid (b), the C12 matrix (c), the NiMo–C12-1 hybrid (d), the C18 matrix (e) and the NiMo–C18-1 hybrid (f).

shifts this band to lower wavenumbers. This suggests a decrease of the side chain conformational disorder[11]. As a result, more efficient hydrophobic interactions can be established between longer side chains, what leads to the better copolymer organization highlighted by XRD results (Figure 2). Indeed, when the copolymer alkyl side chains are longer, a decrease of the full width at half maximum (FWHM) of the copolymer Bragg peak and an increase of the area of this peak are observed[12]. During the calcination of hybrid materials, the more extended copolymer organization promoted by longer alkyl side chains may contribute to liberate a larger and more structured volume for the creation of more pores[13]. Nevertheless, increasing the side chain length could also modify the hydrophobic-hydrophilic balance of the copolymers. As a result, the matrix capacity to remain charged and to interact with polar ions could then be disturbed, making the synthesis of hybrids more difficult. This eventuality is here clarified thanks to a meticulous characterization of hybrids made from copolymers having alkyl side chains of 6, 12 or 18 carbon atoms.

The pK_a values of the two carboxylic functions and of the tertiary amine group of each C6 matrix repeating unit were already estimated between 2–3, 4–5 and 8–9 respectively[7a]. They are listed again in Table 1. Hybrid materials were then prepared

Table 1. pKa of the two carboxylic acids (pKa_1 & pKa_2) and the tertiary amine (pKa_3) of the repeating units of the C6, C12 and C18 matrices.

Copolymer	pKa_1	pKa_2	pKa_3
C6 matrix	2.8 – 4.0	4.5 – 4.7	8.4 – 8.6
C12 matrix	3.0 – 3.2	5.6 – 5.8	8.5 – 8.7
C18 matrix	3.2 – 3.4	6.1 – 6.3	9.7 – 9.9

at pH 6.3-6.5 to maximize the amount of negative COO^- functions (allowing the interaction with the positively charged Ni species) without decreasing the number of positively charged amine moieties (allowing the interaction with negatively charged molybdate species). Such pH window was further adequate as it allows additionally circumventing the low solubility of Ni ions in neutral and basic media from around pH 7. Thereby, the copolymer charge number and thus the copolymer ability to link ions are both maximized. In such conditions, Ni and Mo ions exist as $[Ni(H_2O)_{6-x}(NH_3)_x]^{2+}$ (ionic diameter: 6.3 Å) and MoO_4^{2-} species (ionic diameter: 5.4 Å) respectively[14]. The hybrid materials were prepared without troubling the copolymer organization. Indeed, their synthesis does not induce any disappearance of the copolymer low-angle XRD peak and any shift of the ν_{as}^{CH2} IR band (Figures 2 & 3).

The shift to lower wavenumbers of the COO^- antisymmetric stretching band (ν_{as}^{COO-}) suggests the monodentate coordination of nickel ions by the copolymer COO^- functions (Figure 3)[15]. The addition of Ni and Mo-based ions also shifts the copolymer low-angle XRD peak to lower values: a shift of 0.41, 0.30 and 0.20° is observed for the C6, C12 and C18 matrices respectively (Figure 2). This effect reflects an increase of the copolymer d_{Bragg}: differences $\triangle d_{Bragg}$ of 2.0, 2.9 and 3.0 Å are observed for the C6, C12 and C18 matrices, respectively. By correlating these results, complexation of nickel seems to promote the expansion of the matrix lamellar organization due to the insertion of nickel within the copolymer hydrophilic regions. Besides, the absence of $(NH_4)_6Mo_7O_{24}.4H_2O$ on the hybrid diffractograms suggests a homogeneous dispersion of Mo ions within the matrix[7b]. The over-sized nature of MoO_4^{2-} makes their insertion between the copolymer backbones not plausible. These anions are rather believed to establish electrostatic interactions with the positively charged amines in the intersheet space located in between two copolymer layers[7b]. The d_{Bragg} increase and the ν_{as}^{COO-} band shift are both maximized and stabilized around an I/R ratio = 1 (cfr. exp. section). This suggests the matrix saturation in ions (Figures 4 & 6). The addition of larger ion amounts (I/R ratios > 1) induces the crystallization of $(NH_4)_4[NiMo_6O_{18}(OH)_6]\cdot 5H_2O$ independently of the matrix (Figures S1 & S2), as all further added ions cannot be inserted inside the matrix anymore. Such systems are considered to be heterogeneous.

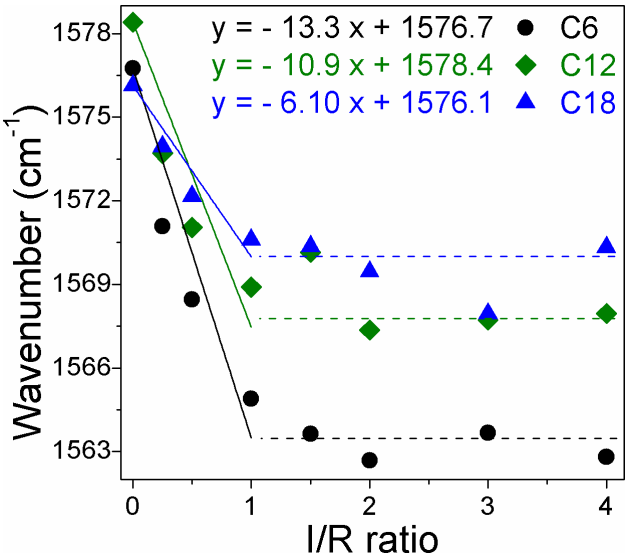

Figure 4. Evolution of the position of the ν_{as}^{COO-} band as a function of the ion amount added to the C6 (black circles), C12 (green diamonds) and C18 matrices (blue triangles). A linear regression is calculated from the ν_{as}^{COO-} band position of materials having an I/R ratio = 0, 0.25, 0.5 and 1.

Positive and negative charges are then crucial to fix both anions and cations to the copolymer. However, the copolymer charge state and the COOH deprotonation especially, appear sensitive to the alkyl side chain length. To evidence this tendency, an area ratio between the ν_{as}^{COO-} band and the carboxyl stretching band of COOH groups ($\nu_{C=O}^{COOH}$, ~1720 cm^{-1}) was calculated ($\nu_{as}^{COO-}/\nu_{C=O}^{COOH}$, Figure 5). It represents a qualitative

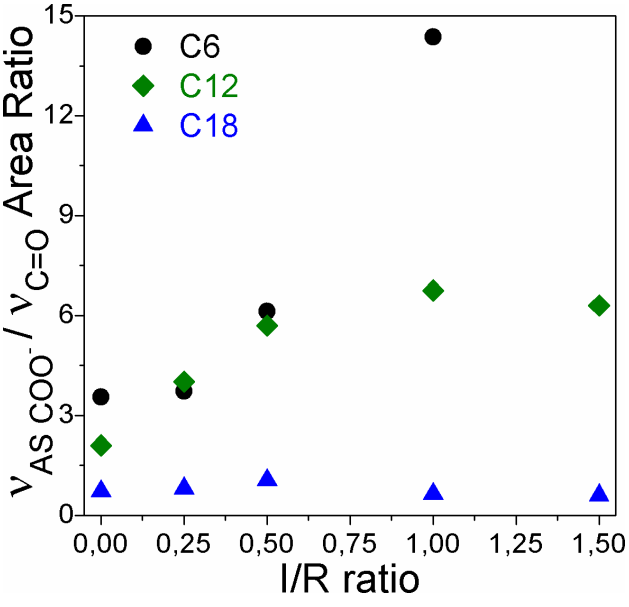

Figure 5. Evolution of the $\nu_{as}^{COO-}/\nu_{C=O}^{COOH}$ area ratio as a function of the amount of Ni & Mo ions added to the C6 (black circles), C12 (green diamonds) and C18 matrices (blue triangles).

tool to compare the amount of deprotonated COOH groups between the three matrices, in presence and in absence of Ni & Mo ions. Under similar acidic conditions (pH 6–6.5), this $\nu_{as}^{COO-}/\nu_{C=O}^{COOH}$ ratio is inversely proportional to the alkyl side chain length. As a result, long alkyl side chains seem to disturb the COOH deprotonation. This deprotonation can be facilitated by the addition of salts[16]. In fact, increasing the charge density of a polymer is easier at high ionic strength thanks to a more effective screening of the pre-existing charges. This is why mixing the C6 matrix with $Ni(NO_3)_2.6H_2O$ and $(NH_4)_6Mo_7O_{24}{\cdot}4H_2O$ in an aqueous solution induces an increase of the $\nu_{as}^{COO-}/\nu_{C=O}^{COOH}$ area ratio. However, this effect is less marked with the C12 matrix and is never observed with the C18 matrix (Figure 5). These FTIR results underline the raising difficulty to confer a net negative charge to copolymers having long alkyl side chains. Titration experiments are in agreement with this assumption (Table 1). Indeed, increasing the length of the copolymer side chains induces a progressive increase of the pK_a of the second COOH function and of the tertiary amine group of each repeating unit. The hydrophobicity of the side chains is likely responsible for this, considering that the deprotonated COO^- group is more polar and thus more hydrophilic than a COOH group[17]. Consequently, increasing the amount of negative COO^- functions within a hydrophobic copolymer matrix is logically unfavorable.

As stated before, the coordination of Ni ions by COO^- functions shifts the ν_{as}^{COO-} band to lower wavenumbers. However, the extent of this shift is inversely proportional to the alkyl side chain length namely 13.3, 10.9 and 6.1 cm^{-1} regarding hybrids (at I/R ratio = 1) coming from the C6, C12 and C18 matrices respectively (Figure 4). This effect would be correlated to the fraction of the COO^- groups that really interacts with nickel ions[15]. In fact the smaller the COO^- fraction linked to nickel is, the smaller the shift will be. As a result, increasing the length of the copolymer alkyl side chains affects the COOH deprotonation but also the ability of this copolymer to bind nickel ions. This statement is confirmed by XRD results and the tendency presented in Figure 6. On this figure, 100% corresponds to the average d_{Bragg} increase of a saturated hybrid. A linear correlation between the d_{Bragg} increase and the amount of ions added to each matrix is also evidenced. Its slope at low I/R ratios proportionally increases with the length of the alkyl side chains. The maximal d_{Bragg} of copolymers having longer side chains is then reached earlier namely when lower ion amounts are mixed with them. More hydrophobic copolymers are thus more rapidly saturated in ions. By correlating XRD and FTIR results, it can be stated that fewer nickel ions can be inserted inside copolymers having longer alkyl side chains as less numerous COO^- groups are available to interact with them. For an I/R ratio = 1, hybrid materials made with the C18 matrix are already heterogeneous as $(NH_4)_4[NiMo_6O_{18}(OH)_6]{\cdot}5H_2O$ is detected. This crystallization is likely facilitated by the labile nature of the Mo – matrix electrostatic bond. At the opposite, those made with the C6 and C12 matrices stay homogeneous.

To summarize, the synthesis of homogeneous and organized hybrids requires the use of copolymers having alkyl side chains that are (i) long enough to confer a regular and ex-

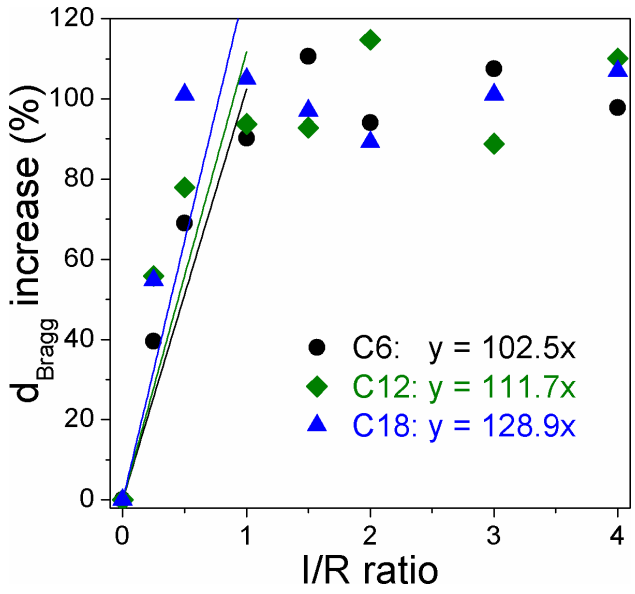

Figure 6. Evolution of the d_{Bragg} increase (expressed in %) as a function the ion amount added to the C6 (black circles), C12 (green diamonds) and C18 matrices (blue triangles). A linear regression is calculated from the d_{Bragg} of materials having an I/R ratio = 0, 0.25, 0.5, 1.

tended organization to the matrix, (ii) but also short enough to limit the unfavorable effect of hydrophobicity on the copolymer ability to remain charged. Thereby, the copolymer capacity to bind inorganic ions is preserved. The C12 matrix then appears as a compromise that offers the possibility to prepare the more extended organized hybrids without actually sacrificing their capacity to fix Ni and Mo-based ions.

Supporting Information Summary

The reader will find in the Supporting Information further details on the preparation protocoles of the different copolymers used and of the hybrid materials. The complete set of X-ray diffractograms of the hybrids are also given for the different copolymers used (varying by the length of their alkyl side chain) and the different I/R ratios. These reveal (i) the increasing level of organization of the materials with the length of the side chain increasing, (ii) the decrease of the angle at which the supramolecular organization of the coplymer diffracts with the increase of the I/R ratio up to IR/ = 1 then its stabilization, going together with (iii) the appearance of non hybridized Ni and Mo in an mixed inorganic salt. SEM pictures are given for the Ni and Mo-containing hybrid (I/R = 1) made with the C18 copolymer. These show the macroscopic lamellar structure.of the material. More details are given on the motivation of our study and approach in the general context of the societal needs for more sustainable chemical processes, in particular those related to the valorization of propane via its oxidative dehydrogenation to propene. Specificities of the different existing polymorphs of Ni molybdates are addressed as well and point to the necessity to develop novative protocoles to prepare the beta polymorph at lower temperature, eventually with a high surface area and a porous structure.

Acknowledgements

The authors gratefully acknowledge the *'Fonds pour la formation à la Recherche dans l'Industrie et dans l'Agriculture (FRIA)'* of Belgium for financial support and B. Farin's PhD fellowship. The authors are also indebted to the '*communauté française de Belgique*' for financial support through the ARC programme (08/13-009).

Keywords: hydrophobicity · host-guest systems · nanostructured materials · polyampholyte · self-assembly

[1] a) C. Sanchez, G. J. d. A. A. Soler-Illia, F. Ribot, T. Lalot, C. R. Mayer, V. Cabuil, *Chem. Mater.* **2001**, *13*, 3061–3083; b) A. B. Descalzo, R. Martínez-Máñez, F. Sancenón, K. Hoffmann, K. Rurack, *Angew. Chem., Int. Ed.* **2006**, *45*, 5924–5948.
[2] B. L. Rivas, E. D. Pereira, I. Moreno-Villoslada, *Prog. Polym. Sci.* **2003**, *28*, 173–208.
[3] M. Vallet-Regi, M. Colilla, B. Gonzalez, *Chem. Soc. Rev.* **2011**, *40*, 596–607.
[4] C. Sanchez, B. Lebeau, F. Chaput, J. P. Boilot, *Adv. Mater.* **2003**, *15*, 1969–1994.
[5] E. Katz, I. Willner, *Angew. Chem., Int. Ed.* **2004**, *43*, 6042–6108.
[6] N. V. Maksimchuk, K. A. Kovalenko, S. S. Arzumanov, Y. A. Chesalov, M. S. Melgunov, A. G. Stepanov, V. P. Fedin, O. A. Kholdeeva, *Inorg. Chem.* **2010**, *49*, 2920–2930.
[7] a) B. Farin, C. Swalus, M. Devillers, E. M. Gaigneaux, *Catal. Today* **2013**, *203*, 24–31; b) B. Farin, P. Eloy, C. Poleunis, M. Devillers, E. Gaigneaux, *Catal. Sci. Technol.* **2016**, *6*, 6046–6056.
[8] a) F. Rullens, M. Devillers, A. Laschewsky, *J. Mater. Chem.* **2004**, *14*, 3421–3426; b) F. Rullens, N. Deligne, A. Laschewsky, M. Devillers, *J. Mater. Chem.* **2005**, *15*, 1668–1676.
[9] K. Inomata, Y. Sakamaki, T. Nose, S. Sasaki, *Polym. J. (Tokyo, Jpn.)* **1996**, *28*, 992–999.
[10] D.-S. Wang, T. Xie, Q. Peng, S.-Y. Zhang, J. Chen, Y.-D. Li, *Chem. - Eur. J.* **2008**, *14*, 2507–2513.
[11] R. Suresh, N. Venkataraman, S. Vasudevan, K. V. Ramanathan, *J. Phys. Chem. C* **2006**, *111*, 495–500.
[12] S. Sinha Ray, M. Okamoto, *Prog. Polym. Sci.* **2003**, *28*, 1539–1641.
[13] a) M. Widenmeyer, R. Anwander, *Chem. Mater.* **2002**, *14*, 1827–1831; b) J. Wei, Y. Deng, J. Zhang, Z. Sun, B. Tu, D. Zhao, *Solid State Sci.* **2011**, *13*, 784–792.
[14] a) B. Beverskog, I. Puigdomenech, *Corros. Sci.* **1997**, *39*, 969–980; b) L. E. Briand, G. M. Valle, H. J. Thomas, *J. Mater. Chem.* **2002**, *12*, 299–304; c) K.-H. Goh, T.-T. Lim, Z. Dong, *Water Res.* **2008**, *42*, 1343–1368.
[15] T. J. Strathmann, S. C. B. Myneni, *Geochim. Cosmochim. Acta* **2004**, *68*, 3441–3458.
[16] O. Colombani, E. Lejeune, C. Charbonneau, C. Chassenieux, T. Nicolai, *J. Phys. Chem. B* **2012**, *116*, 7560–7565.
[17] a) M. Uchman, K. Procházka, M. Štěpánek, G. Mountrichas, S. Pispas, M. Špírková, A. Walther, *Langmuir* **2008**, *24*, 12017–12025; b) M. Vermathen, E. A. Louie, A. B. Chodosh, S. Ried, U. Simonis, *Langmuir* **1999**, *16*, 210–221.

Submitted: June 7, 2016
Accepted: August 23, 2016